Atmospheric Environment Vol. 12, pp. 1981–1990.

0004-6981/78/1001-1981 $02.00/0

CALCULATED PARTICLE COLLECTION EFFICIENCIES BY SINGLE DROPLETS CONSIDERING INERTIAL IMPACTION, BROWNIAN DIFFUSION AND ELECTROSTATICS

ANIL PREM and MICHAEL J. PILAT
Department of Civil Engineering, University of Washington, Seattle, WA 98195, U.S.A.

(*First received* 22 *August* 1977 *and in final form* 10 *February* 1978)

Abstract – Particle collection efficiencies in the size range of 0.1–20 μm dia. by a single droplet, were calculated using Runge–Kutta numerical solution techniques for the particle equation of motion. Calculations were done for two droplet diameters, 50 and 200 μm with sedimentation velocities of 7.55 and 100 cm s^{-1} respectively. The droplets and the particle gas stream were assumed to be at 38°C. In all the calculations, the particle was assumed to be charged negative and the droplet charged positive. The collection mechanisms considered were the inertial impaction, Brownian diffusion and electrostatic forces. The electrostatic forces considered were the Coulombic force of attraction between the droplet and particle, the charged-particle image force and the charged-collector image force. From the calculations it was observed that among the electrostatic forces, the Coulombic force of attraction was the predominant force. The calculations predicted that in the 0.1–20 μm dia. particle range, the collection efficiencies were significantly increased when electrostatic forces were added. The calculations also predicted that when electrostatic forces were present, the 50 μm dia. droplet gave much higher collection efficiencies than the 200 μm dia. droplet for the particle size range considered.

NOMENCLATURE

a	radius of corona wire
A	acceleration of the particle
b	wire to plate spacing in the particle charging equipment
C	Cunningham correction factor
C_∞	particle concentration outside the stagnant layer
CE	critical corona field
D	droplet diameter
D_B	Brownian diffusivity of particles
D_p	particle diameter
e	electron charge
E_c	corona discharge electric field strength for charging the droplet
E_0	corona discharge electric field strength for charging the particle
F_{Brownian}	Brownian force on the particle
F_c	Coulombic force of attraction between the particle and droplet
F_{drag}	drag force on the particle
$F_{\text{ext}-x}$	sum of external forces in X-direction
$F_{\text{ext}-y}$	sum of external forces in Y-direction
F_{ID}	droplet image force
F_{IP}	particle image force
$F(t)$	sum of forces on the particle
i	corona current in the particle charging equipment
j	current density in the particle charging equipment
k	Boltzman constant
K	Stokes number
KC	electrostatic parameter due to Coulombic force
m	mass of an air molecule
m_p	mass of the particle
M	gas molecular weight
N_0	free ionic density
P	total gas pressure
$q(t)$	charge on particle due to diffusion charging
Q_c	saturation charge on droplet due to field charging
Q_p	saturation charge on particle due to field charging
R	ideal gas constant
R_d	droplet radius
R_p	particle radius
Re	Reynolds number of the droplet
$\mathscr{R}$	distance between the centers of the droplet and particle
Sc	Schmidts number of the diffusing aerosol particles
t	time of diffusion charging (s)
T_g	temperature of gas
u	fluid velocity
U_0	undisturbed fluid velocity, same as the free fall speed of the droplet
U_x	nondimensional fluid velocity in X-direction
U_y	nondimensional fluid velocity in Y-direction
v	root mean square velocity of gas molecules
v_p	particle velocity
V	applied voltage for the particle charging equipment
V_B	particle velocity due to Brownian diffusion
V_0	corona starting voltage
V_x	nondimensional particle velocity in X-direction
V_y	nondimensional particle velocity in Y-direction
X	nondimensional distance in X-direction
ΔX_B	film thickness surrounding the droplet for particle Brownian diffusion
Y	nondimensional distance in Y-direction
Y_0	initial Y position measured from the drop centerline of the particle trajectory that just grazes the droplet

Greek letters

δ	relative air density
ε	relative permittivity of particles
ε_c	dielectric constant of droplet
ε_0	dielectric constant of air

ε_p dielectric constant of particle
η' single droplet collection efficiency
ρ_g density of gas
θ angle that the line joining the center of the particle to the center of the droplet makes with the drop centerline
μ ion mobility
μ_g viscosity of gas.

I. INTRODUCTION

With the present interest in fine particulate collection at moderate costs, the trend in the current fine particulate control includes using collection mechanisms other than particle inertia. Electrostatic precipitators, high pressure scrubbers and bag filters had been used for fine particulate control. The latter two have high operating costs whereas electrostatic precipitators have high capital cost. Electrostatic scrubbers have been shown to be efficient fine particulate collectors. The apparent advantage of using wet electrostatic scrubbers is the low capital and operating costs, and simultaneous collection of particles and gases.

Kramer and Johnstone (1955) calculated the single droplet collection efficiencies, but they only considered the electrostatic forces; particle inertia and Brownian diffusion were neglected. Pilat *et al.* (1974) reported the calculation of single droplet collection efficiencies considering the inertial impaction, Brownian diffusion and electrostatic mechanisms. George and Poehlein (1974) presented a model for collection of single droplet collection efficiencies of particles using particle inertia and electrostatic forces. Nielsen and Hill (1976) presented some single droplet collection efficiency calculations using particle inertia and electrostatic forces. Potential flow and Stokes flow were used to model the gas flow around the droplet. They concluded that electrical forces enhance particle collection and the effect of electrical forces reach a maximum for negligible particle inertia.

Studies on the growth of cloud droplets into rain drops have involved the consideration of collisions of charged droplets in electric fields. Moore and Vannegut (1960) reported that electric fields may have a very appreciable effect in accelerating the coalescence process in clouds. Sartor (1960) calculated electrostatic forces and collision efficiencies for two droplet pairs in electric fields ranging from 14 to 2000 V cm^{-1}. The calculations were done assuming the hydrodynamic collision efficiency as zero (no inertial forces). He concluded that the electric fields significantly affect the rate of collision and coalescence of cloud droplets. Lindblad and Semonin (1963) and Plumlee and Semonin (1965) calculated collision efficiencies of uncharged droplets in electric fields and concluded that the collision efficiency for a given pair of droplets increases as the applied electric field increases. Semonin and Plumlee (1966) reported collision efficiency calculations for charged droplets in electric fields. They concluded that the electric effects influence collision efficiencies only when the droplet charges were greater than 10^{-16} C or when the electric field intensity exceeded 900 V cm^{-1}. Paluch (1970) derived analytical expressions for collision efficiencies between drop–droplet pairs. Based on the calculated electrostatic collision efficiencies and using the derived analytical expressions, empirical approximation formulas were arrived at for a limited number of drop–droplet pair sizes and electrical conditions. Sartor (1970) calculated collision efficiencies for drop–droplet pairs considering the influence of charges and electric fields found in clouds. These were incorporated into instantaneous mass accretion rate calculations. He concluded that the droplet diameter can be increased by an order of magnitude by electric forces when all droplets involved are less than 100 μm. The effect decreases with increasing droplet size.

In the existing literature we were unable to find any work that clearly addressed the problem of collision efficiencies of droplets with particles (0.1–20 μm dia.) emitted from industrial sources considering inertial impaction, Brownian diffusion and electrostatic forces when the droplets and particles are oppositely charged. This paper attempts to present the mathematics for the charging mechanisms for particles and droplets and a simple model to calculate particle efficiencies by a single droplet when inertial impaction, Brownian diffusion and electrostatic forces due to oppositely charged particles and droplets are present in a scrubber. Calculations were done to study the effect of electrostatic forces and droplet size on the collection efficiencies of particles in the size range of 0.1–20 μm.

II. SINGLE DROPLET COLLECTION EFFICIENCY CALCULATION

(a) *Definition of single droplet collection efficiency*

The particle collection efficiency η of a single droplet can be given by

$$\eta = \frac{(Y_0 + R_p)^2}{R_d^2} \tag{1}$$

where Y_0 is the initial Y position (measured from the drop center-line) of the particle center trajectory that just grazes the droplet, R_p, the particle radius and R_d, the droplet radius. These parameters are illustrated in Fig. 1. Note that the droplet collection efficiency defined in Equation (1) considers the finite size of the particle (to obtain the area swept free of particles). The Y_0 is calculated using the particle equation of motion for a gas flowing around a spherical droplet.

(b) *Equation of particle motion*

The X and Y components of the equation of particle motion (developed in the Appendix) are

$$\frac{d^2X}{dT^2} = \frac{1}{2K}(U_x - V_x) - \frac{F_{ext-x} - R_d}{m_p U_0^2}, \tag{2}$$

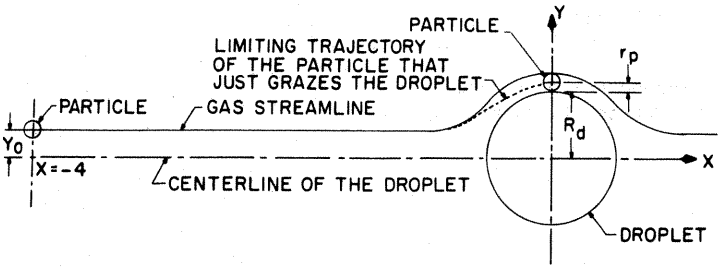

Fig. 1. Schematic of the model used for calculating single droplet collection efficiencies.

$$\frac{d^2Y}{dT^2} = \frac{1}{2K}(U_y - V_y) - \frac{F_{ext-x} - R_d}{m_p U_0^2}, \quad (3)$$

where X and Y are non-dimensional distances, T, non-dimensional time, K, the Stokes number

$$\left(K = \frac{C\rho_p U_0 R_p^2}{9\mu_g R_d}\right),$$

U_x and U_y the non-dimensional fluid velocity components, V_x and V_y, the non-dimensional particle velocity components, F_{ext-x} and F_{ext-y} are X and Y, components of the sum of the external forces on the particle, R_d, the droplet radius, m_p, the mass of the particle, U_0, the undisturbed fluid velocity, C, the particle Cunningham correction factor and μ_g, the fluid viscosity. After substituting in the initial condition ($X = -4.0$, $T = 0$ and $Y = Y_0$), the appropriate fluid velocity flow field (U_x and U_y) and the external particle forces (F_{ext-x} and F_{ext-y}), Equations (2) and (3) can be solved using a Runge–Kutta numerical technique.

(c) *Fluid flow field*

For all the calculations the fluid flow was assumed to be potential. For potential flow U_x and U_y are given by

$$U_x = 1 - \frac{2X^2 - Y^2}{2(X^2 + Y^2)^{2.5}}, \quad (4)$$

$$U_y = \frac{-3XY}{2(X^2 + Y^2)^{2.5}}. \quad (5)$$

(d) *Charge on particles and droplets*

Particles and droplets are electrostatically charged in coronas by two mechanisms; field charging and diffusion charging. Field charging is the dominant mechanism for large particles with a diameter greater than about 0.5 μm, while diffusion charging predominates for small particles with a diameter less than about 0.2 μm. Field charging is related to the ordered motion of ions under the influence of an applied electric field. This ordered motion causes collisions between the ions and the particles suspended in the gas stream. Diffusion charging results from ionic collisions with the particles brought about by the random thermal motion of the ions in the gas. Olgesby *et al.* (1970) report the saturation charge Q_c on the collector droplet due to field charging as

$$Q_c = 12\pi\varepsilon_c\varepsilon_0 R_d^2 E_c/(\varepsilon_c + 2\varepsilon_0) \quad (6)$$

where ε_c is the dielectric constant of drop assumed to be $80\varepsilon_0$, ε_0, the dielectric constant of air, R_d, the radius of the droplet and E_c, the corona discharge electric field strength for charging the droplet. Similarly, the saturation charges on the aerosol particle Q_p due to field charging is given by

$$Q_p = 12\pi\varepsilon_p\varepsilon_0 R_p^2/(\varepsilon_p + 2\varepsilon_0), \quad (7)$$

where ε_p is the dielectric constant of the particle and E_0, the corona discharge electric field strength for charging the particle.

Olgesby *et al.* (1970) report the time dependent diffusion charging of a particle $q(t)$ as

$$q(t) = \frac{R_p kT_g}{e} \ln\frac{(1 + \pi R_p v N_0 e^2 t)}{kT_g} \quad (8)$$

where $q(t)$, the charge on particle is in Coulombs, k is the Boltzmann constant, T_g, temperature of gas, v, the root mean square velocity of gas molecules, e, the electron charge, R_p, the particle radius and N_0, the free ionic density. The root mean square velocity of gas molecules v is given by

$$v = \left(\frac{8kT_g}{\pi m}\right)^{1/2} \quad (9)$$

where m is the mass of an air molecule.

White (1963) reports the free ionic density N_0 as

$$N_0 = j/e\mu E_0 \quad (10)$$

where j is the current density, μ, the ion mobility and E_0, the applied voltage.

All the variables in Equation (8) are known; they are either constants or particle charging equipment operating variables. The only term that is not known is the current density j.

The particle charging equipment considered was the wire and plate type. By definition, current density is the corona current flowing across unit cross-section area. In a wire-plate particle charging equipment, the average current density across the inter-electrode space is equal to the current density at the plates.

$$j = \frac{\text{Corona current } (i)}{\text{Plate area}}. \quad (11)$$

Now in order to calculate current density the corona current has to be calculated. This can be best done by

getting the voltage–current characteristics experimentally. When this is not possible, the corona current (i) can be approximated theoretically. The corona current i is a function of applied voltage, electrode geometry, gas composition, gas temperature and pressure, particulate matter in gas and on the electrodes, and the physical properties of the particulate matter.

There are many empirical equations for calculating corona current (i) from the applied voltage for the wire tube particle charging equipment, but not many for wire-plate configuration. White (1963) however, does give an equation for calculating the corona current per unit length of the wire.

$$\frac{\text{Corona current}}{\text{Unit length of wire}} = \frac{\mu}{b^2 \log(4b/\pi a)} V(V - V_0) \quad (12)$$

where V is the applied voltage, V_0, the corona starting voltage, b, the wire to plate spacing and a wire radius. Equation (12) is valid only when the wire to wire spacing is greater than the wire to plate spacing.

White (1963) reports the corona starting voltage V_0 as

$$V_0 = aCE \log\left(\frac{\pi a}{2b}\right) \quad (13)$$

where CE, the critical corona field, is given by

$$CE = 30\delta + 9\sqrt{\delta/a} \quad (14)$$

where δ, the relative air density, is given by

$$\delta = \left(\frac{293}{T_g}\right)\left(\frac{P}{760}\right) \quad (15)$$

where T_g and P are the gas temperature in Kelvin and gas pressure in mm of mercury respectively.

Corona current i is obtained by multiplying the corona current per unit length of wire from Equation (12) by the length of the wire.

(e) *External forces on particles*

1. *Brownian diffusion.* Using the Stokes–Cunningham equation, the pseudo-force on an aerosol particle due to its Brownian diffusion is given as

$$F_{\text{Brownian}} = \frac{6\pi\mu_g R_p V_B}{C} \quad (16)$$

where V_B is the particle velocity toward the droplet due to the existing particle concentration gradient around the droplet and is not the instantaneous velocity of the particle undergoing a zig-zag Brownian motion. In calculating the particle velocity due to Brownian diffusion V_B, it is assumed that the particles reach the droplet surface entirely by diffusion through a stagnant layer surrounding the droplet. The thickness of the layer is a function of the shape of the droplet, properties of the gas and diffusing species and the gas velocity. Or in other words, the velocity calculations are done in a manner analogous to the rate of absorption of a solute gas from a gas mixture. In the calculations it is assumed that the concentration of aerosol particles remains uniform outside the stagnant layer, while as at the droplet surface the equilibrium particle concentration is zero (i.e. all the particles that strike the droplet surface are collected by the droplet).

From the consideration of osmotic forces, Einstein (1908) derived the following expression for the mass transfer of a solute in a solution due to diffusion in a concentration gradient

$$V_B C_\infty = -D_B \frac{dc}{dx} \quad (17)$$

where V_B is the velocity of the solute molecule, C_∞, the concentration of solute molecules, D_B, the diffusivity of the solute molecules and dc/dx is the concentration gradient of the solute molecules.

Movement of particles due to diffusion in gas where particle concentration gradient exists can be calculated using Equation (17). In our model the concentration of particles outside the stagnant layer surrounding the droplet is uniform and is equal to C_∞. Within the stagnant layer of thickness ΔX_B, there exists a linear particle concentration gradient resulting in the diffusion of particles toward the droplet surface where the particle concentration is zero. Therefore the particle concentration gradient across the stagnant layer reduces to

$$\frac{dc}{dx} = \frac{C_{\text{Bulk gas}} - C_{\text{Droplet surface}}}{\text{Stagnant layer thickness}} = \frac{C_\infty - 0}{\Delta X_B}. \quad (18)$$

Substituting Equation (18) for the concentration gradient in Equation (17) gives the velocity of the diffusing particle V_B in the stagnant layer surrounding the droplet as

$$V_B C_\infty = D_B \frac{(C_\infty - 0)}{\Delta X_B} \quad (19)$$

or

$$V_B = D_B/\Delta X_B. \quad (20)$$

Johnstone and Roberts (1949) and Ead (1948) reported the boundary layer thickness ΔX_B due to mass transfer of particles as

$$\Delta X_B = D/(2 + 0.557\,\mathrm{Re}^{0.5}\,\mathrm{Sc}^{0.375}) \quad (21)$$

where Re is the Reynolds number of the droplet and D is the droplet diameter. The Schmidt number of aerosol particles Sc is given as

$$\mathrm{Sc} = \mu_g/\rho_g D_B \quad (22)$$

where μ_g is the gas viscosity, ρ_g, the gas density and D_B, the particle diffusivity.

For particles of diameter greater than the gas mean free path of 0.062 μm the particle diffusivity was calculated using the equation reported by Einstein (1908)

$$D_B = \frac{CkT_g}{6\pi\mu_g R_p} \tag{23}$$

where T_g is the gas temperatue and k the Boltzmann constant. For particles of diameter less than the gas mean free path, the particle diffusivity was calculated using Langmuir's (1942) equation based on Stephen–Maxwell diffusion theory

$$D_B = \frac{4kT_g}{3\pi D_p^2 P}\left(\frac{8RT_g}{\pi M}\right)^{1/2} \tag{24}$$

where D_p is the particle diameter, P, the total gas pressure, R, the ideal gas constant and M, the gas molecular weight.

2. *Electrostatic forces.* The electrostatic forces considered in the model were (a) the Coulombic force between the point charges of magnitude Q_p and Q_c located at the center of the particle and droplet, respectively, (b) the particle image force on the neutral droplet and (c) the collector image force on the neutral particle. The Coulombic force between a charged particle and a charged droplet is given by

$$F_c = -\frac{Q_c Q_p}{4\pi\varepsilon_0 \mathscr{R}^2} \tag{25}$$

where Q_c and Q_p are the charges on the droplet and particle, respectively, ε_0 is the dielectric constant of air and $\mathscr{R}$ is the distance between the centers of the particle and droplet.

Kramer and Johnstone (1955) reported the particle image force F_{IP} as

$$F_{IP} = -\left(\frac{\varepsilon_c - 1}{\varepsilon_c - 2}\right)\frac{Q_p^2 R_d}{4\pi\varepsilon_0}\left[\frac{1}{\mathscr{R}^3} - \frac{\mathscr{R}}{(\mathscr{R}^2 - R_d^2)^2}\right] \tag{26}$$

where ε_c is the relative permitivity of the droplet which is equal to 80 for water droplets, Equation (26) is reduced to

$$F_{IP} = -\frac{Q_p^2 R_d}{4\pi\varepsilon_0}\left[\frac{1}{\mathscr{R}^3} - \frac{\mathscr{R}}{(\mathscr{R}^2 - R_d^2)^2}\right] \tag{27}$$

Kramer and Johnstone (1955) reported the collector-image force F_{ID} as

$$F_{ID} = \left(\frac{\varepsilon_p - 1}{\varepsilon_{p+2}}\right)\frac{Q_c^2 R_p^3}{2\pi\varepsilon_0 \mathscr{R}^5} \tag{28}$$

where ε_p is the relative permitivity of the particles and is equal to 5.

(e) *Computer program for calculating single droplet collection efficiencies*

A computer program calculated the limiting trajectory of the particles that just grazes the droplet, which in turn was used to calculate the single droplet collection efficiency. The main program calculated the settling velocities of the particles and droplet, film thickness surrounding the droplet in which Brownian diffusion is active, Brownian forces on the particles and charge on the collector. The charges on the particles are calculated in a subroutine which is called in the main program. The constants for the electrostatic forces and electrostatic parameters are also calculated in the main program.

A subroutine calculated the charge on the particle. For particles larger than 0.1μm radius, the charge is calculated by the field charging mechanism and for particles less than or equal to 0.1 μm radius the charge is calculated by the diffusion charging mechanism. Another subroutine calculated the limiting trajectory of the particle that just grazes the droplet, which in turn was used to calculate the single droplet collection efficiency. The particle trajectory was calculated by stepsize iteration of the equations of motion of the particles using a 4th order Runge–Kutta process. This was done by calculating the forces on the particle and allowing it to move for a small increment of time after which the forces on the particle were recalculated. Since it was assumed that the forces on the particles were constant during the small increment of time, the selection of the increment of time was very important. The size of the time increment or stepsize was calculated by considering the radius of curvature of the particle trajectory. The greater the curvature, the smaller the stepsize. The radius of curvature of the particle trajectory is an indication of the direction of the forces and the change in the magnitude of the forces acting on the particle. The stepsize was calculated by assuming a constant subtended angle between the successive location points on the particle trajectory. Therefore, when the trajectory was straight, the time increment was large, but when the trajectory was curved, the stepsize was decreased depending on the curvature of the particle trajectory.

In the calculations the Brownian forces exist only within a thin film surrounding the droplet. The efficiency calculations were done considering both the front and the back side of the droplet. Once the limiting trajectory for a given particle diameter was calculated, the single droplet collection efficiency of the particle computed. The calculations were then repeated for another particle diameter. This continued until calculations for all the particle sizes of interest were completed.

III. DISCUSSION AND RESULTS

(a) *Calculated particle and droplet charge*

The calculated droplet charge to mass ratio for the droplet diameter of 50 μm with applied electric field of 1000 and 5000 V cm^{-1} was 3.11×10^{-7} and 1.55×10^{-6} C gm^{-1}, respectively. The charge to mass ratio for the 200 μm dia. droplet with applied electric field of 1000 and 5000 V cm^{-1} was 0.78×10^{-7} and 0.39×10^{-6} C gm^{-1}, respectively. Figure 2 illustrates the calculated particle charge/mass ratio for the applied electric fields of 1000 and 5000 V cm^{-1}.

(b) *Effect of various forces in the particle size range considered*

A very convenient way of comparing the magni-

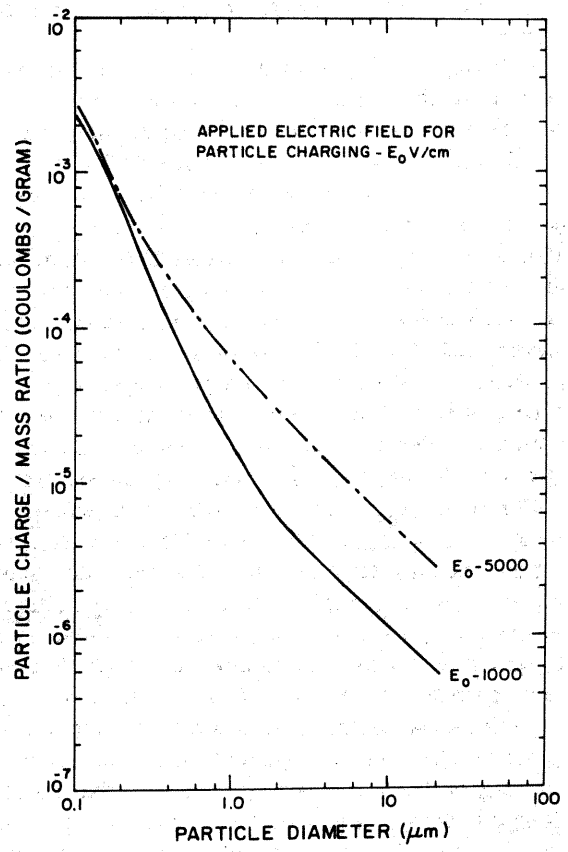

Fig. 2. Plot between the particle dia. and particle charge to mass ratio for applied electric fields of 1000 and 5000 V cm^{-1}.

tudes of forces acting on the particles is to convert the forces into dimensionless numbers. This could be done by first expressing all the forces into dimensionless terms and then by dividing all these by a common dimensionless denominator. Generally this denominator is the particle drag. The forces used in the calculations were inertial impaction, Brownian diffusion and electrostatic forces. In the particle size range considered (0.1–20 μm), the Brownian diffusion is negligible and so it is excluded from this comparison of forces. The dimensionless number representing the inertial force on the particle is the Stokes number K. The Stokes number is given by

$$K = \frac{C\rho_p U_0 R_p^2}{9R_d\mu_g}. \tag{29}$$

The electrostatic forces considered in the model were Coulombic, particle-image and collector image. The calculations predicted that compared to Coulombic force, particle-image and collector image forces were negligible. Therefore, the dimensionless electrostatic parameter KC was calculated using only the Coulombic force of attraction between the droplet and particle. Nielsen (1974) reports the dimensionless electrostatic parameter KC as

$$KC = \frac{Q_c Q_p C}{24\pi^2\varepsilon_o\mu_g R_p U_o R_d^2}. \tag{30}$$

Figures 3 and 4 illustrate the relative magnitudes of inertial and electrostatic forces on the particle size range of 0.1–20 μm. The electrostatic calculations were done for two sets of charging conditions: (1) droplet and particles charged oppositely in a corona of 1000 V cm^{-1} and (2) droplet and particles charged oppositely in a corona of 5000 V cm^{-1}. Since the Stokes number is not affected by the electrostatic forces, comparison of the Stokes number and electrostatic parameter for a given charging condition would give us an indication of the effect of inertial and electrostatic forces on the collection of a given particle.

The relative magnitude of the dimensionless number of any specific collection mechanism is a good indication of its relative influence on the collection of particles. For example, if from Fig. 3 it is found that for a specific particle size the Stokes number is numerically larger than the electrostatic parameter, it indicates that for the collection of that size particle by a 200 μm dia. droplet, particle inertia is more significant than the electrostatic forces on the particle.

It should be noted that both the inertial and electrostatic forces are additive on the front-half of the droplet; that is, they both bring the particle closer to the droplet aiding collection. Whereas on the backside of the droplet with a potential fluid flow field, the electrostatic force aids collection and the particle inertia hinders collection. This occurs because the electrostatic force always acts towards the center of the droplet, but particle inertia takes the particle away

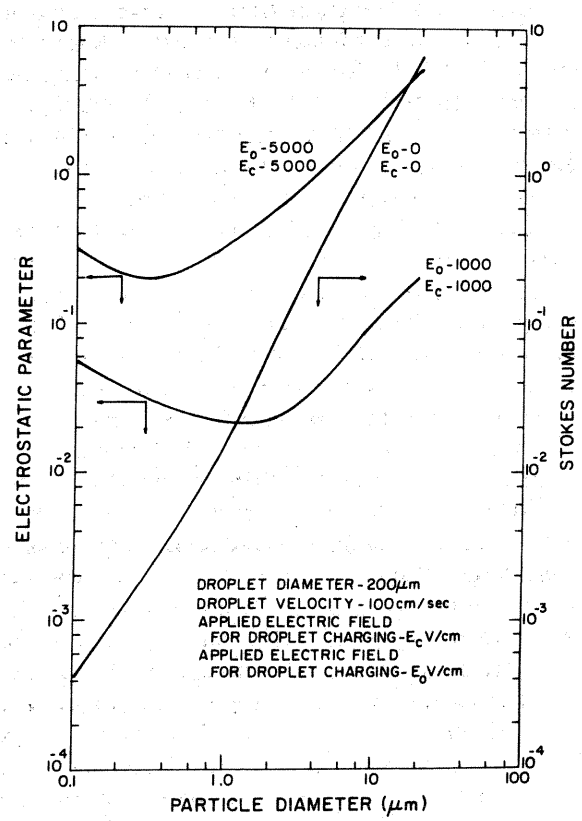

Fig. 3. Plot between the particle size and, electrostatic parameter and Stokes number for a 200 μm dia. droplet.

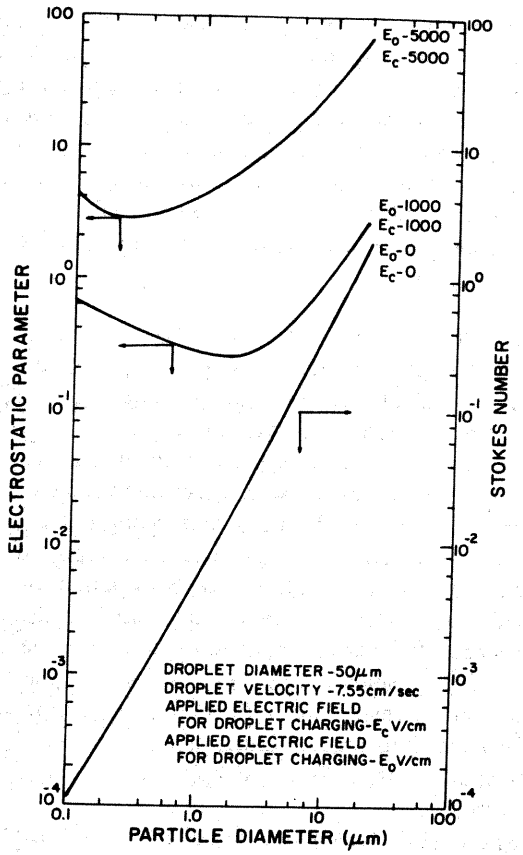

Fig. 4. Plot between the particle size and, electrostatic parameter and Stokes number for a 50 μm dia. droplet.

from the droplet on the back-side of it. Thus, for larger particles having a significant Stokes number compared to the electrostatic parameter, the particle collection on the back-half side of the droplet is negligible compared to the front half. However, for small particles having a small Stokes number compared to the electrostatic parameter, the particle collection on the backside of the droplet can be significant.

Referring to Fig. 3 with a 200 μm droplet, let us compare the Stokes number and the electrostatic parameter curves, where the droplet and particles are charged oppositely in a corona of 1000 V cm^{-1}. It can be seen that for particles greater than 1.2 μm dia., the Stokes number is larger than the electrostatic parameter, indicating that for the collection of particles in this size range, particle inertia is the dominant collection mechanism compared to electrostatic forces. But for the collection of particles smaller than 1.2 μm dia., since the electrostatic parameter is numerically larger than the Stokes number, electrostatic forces are the dominant collection mechanism compared to particle inertia. Referring to Fig. 3 again, comparing the electrostatic parameter and Stokes number curves when the droplet and particle are charged oppositely in a corona of 5000 V cm^{-1}, it can be seen that for particles between 10 and 20 μm dia. both the electrostatic forces and particle inertia are comparable. But for particles smaller than 10 μm dia., the electrostatic forces progressively become the dominant collection mechanism compared to particle inertia.

Referring to Fig. 4 with a 50 μm dia. droplet, comparing the Stokes number and the electrostatic parameter curves when both the droplet and particles are charged oppositely in a corona of 1000 V cm^{-1}, it can be seen that for particles larger than 10 μm dia. particle inertia and electrostatic forces are comparable. However, for particles smaller than 10 μm dia., the electrostatic forces progressively become the dominant collection mechanism compared to particle inertia. Referring to Fig. 4 again, when both the particles and droplet are charged oppositely in a corona of 5000 V cm^{-1}, the electrostatic forces are the dominant collection mechanism compared to particle inertia in the whole particle size range considered.

Comparing Figs 3 and 4 for a specific particle size, it is seen that for the same droplet and particle charging conditions, the electrostatic forces are more dominant for the 50 μm dia. droplet compared to the 200 μm dia. droplet. This effect can be explained by looking at Equation 30 for the electrostatic parameter. For the same particle size and particle and droplet charging conditions, the electrostatic parameter is a function of droplet size, droplet charge, and the free fall speed of the droplet. From Equation (6), it is seen that droplet charge is directly proportional to the square of the droplet size. Therefore the electrostatic parameter becomes a function of only the droplet free fall speed V_0. The smaller the free fall speed of the droplet, the higher the electrostatic parameter. Physically, this indicates that when the droplet free fall speed is smaller, the particle spends a longer time near a given droplet, and thus the electrostatic forces between the droplet and particle act for a longer duration of time, enhancing the particle collection.

(c) *Calculated single droplet collection efficiencies*

The calculated particle collection efficiencies of 200 and 50 μm dia. droplets are presented in Figs 5 and 6 respectively. The calculations were done for the following cases: (1) considering only particle inertia and Brownian diffusion, electrostatic forces absent; (2) considering particle inertia, Brownian diffusion and particle and droplet charged oppositely in a corona of 1000 V cm^{-1} and (3) considering particle inertia, Brownian diffusion and particle and droplet charged oppositely in a corona of 5000 V cm^{-1}.

Referring to Fig. 5, comparing the two collection efficiency curves, when electrostatic forces are absent, and when the particles and droplet are charged oppositely in a corona of 1000 V cm^{-1} it is seen that the particle collection efficiency increased over all the particle size range, but the increase is more significant for particles smaller than 1.2 μm dia. For example, whereas for a 20 μm dia. particle, the fractional collection efficiency increased from 1.33 to 1.41 when electrostatic forces were added, the increase in collection efficiency for a 0.1 μm dia. particle was from 0.0033 to 0.227. The reason for this significant increase

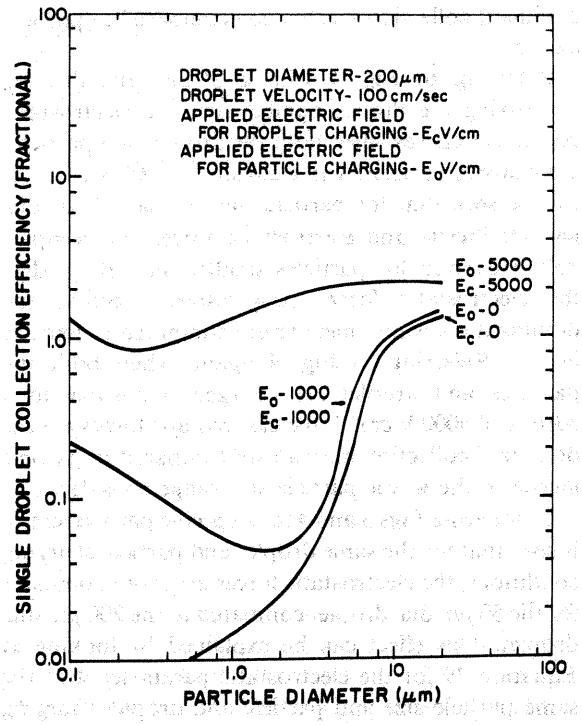

Fig. 5. Calculated particle collection efficiencies of a single 200 μm dia. droplet at 100 cm s^{-1} velocity at various electric field strengths.

in the particle collection efficiency for particles smaller than 1.2 μm dia. can be explained by referring to Fig. 3, where it is seen that for these smaller particles the electrostatic forces are very dominant compared to the inertial forces, the result being being than when these electrostatic forces are added to particle inertia and Brownian diffusion, the particle collection efficiency significantly increases. The extent to which the particle collection efficiency increases depends on the extent to which the electrostatic forces are increased on the particle. This can be seen by looking at the collection efficiency curve when both the particle and droplet are charged oppositely in a corona of 5000 V cm^{-1}.

Let us now consider the 50 μm dia. droplet. Comparing the two collection efficiency curves, when electrostatic forces are absent and when the particle and droplet are charged oppositely in a corona of 1000 V cm^{-1}, it is seen that the particle collection efficiency increases over the complete particle size range considered when electrostatic forces are added. The increase in particle collection efficiency for the 50 μm dia. droplet is more significant than for the 200 μm dia. droplet for the same particle and droplet charging condition. The reason for this has already been explained earlier. The particle collection efficiency is even further increased when the droplet and particle are charged oppositely in a corona of 5000 V cm^{-1}.

From the results it is seen that the particle collection efficiency is a function of Stokes number and electrostatic parameter. When particle inertia is the dominant collection mechanism as seen from the case when electrostatic forces are absent, the collection efficiency curve resembles the curve for the Stokes number. But when electrostatic forces become predominant, the particle collection efficiency curve resembles the electrostatic parameter curve. When both the electrostatic forces and particle inertia are active, the particle collection efficiency curve is affected both by the electrostatic parameter curve and the Stokes number curve.

(d) *Comparison with reported results*

The computer model for single droplet collection efficiency calculations was earlier compared by Pilat and Prem (1976) and was found to be in good agreement with results reported in the literature. Our results were compared with experimental collection efficiencies reported by Ranz and Wong (1952), empirical efficiencies from the equation reported by Johnstone and Roberts (1949) for Brownian diffusion, Fonda and Herne's (1960) calculated collection efficiencies for inertial impaction with a potential gas flow field, Spark's (1971) calculated collection efficiencies considering both inertial impaction and Brownian diffusion, and Langmuir's (1948) calculated efficiencies with a 100 μm droplet and potential gas flow field.

Sparks (1971) calculated the collection efficiency of a 200 μm dia. droplet with a free fall speed of 100 cm s^{-1}, considering inertial impaction, Brownian diffusion and electrostatic forces. The electrostatic forces considered were the same as in this paper. The droplet and particle were charged oppositely in a corona of

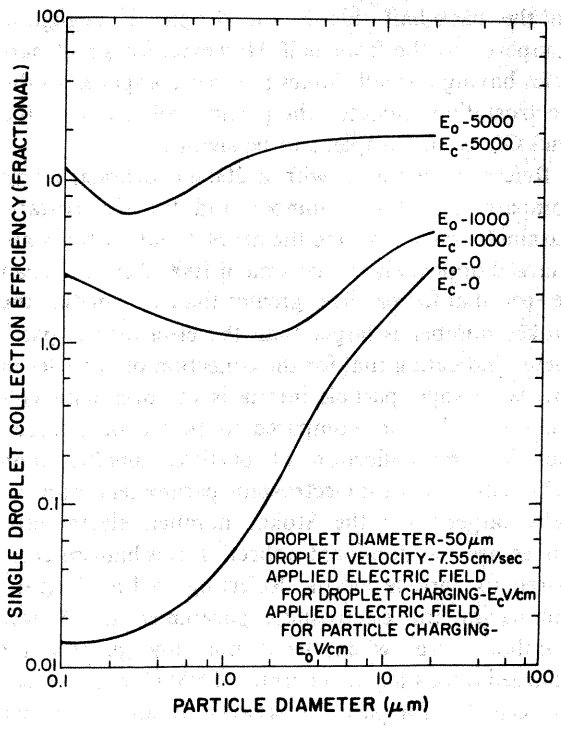

Fig. 6. Calculated particle collection efficiencies of a single 50 μm dia. droplet at 7.55 cm s^{-1} velocity, at various electric field strengths.

1000 V cm^{-1}. From his plot between particle size and collection efficiencies, the collection efficiencies obtained for small particles are very high. For example, for a 0.1 μm dia. particle, Sparks reports a collection efficiency of 275%, whereas we get 22.7%. For a particle diameter of 1.0 μm, Sparks reports a collection efficiency of 160%, whereas our value is around 5%. For a particle diameter of 20 μm there was no change in the collection efficiency in Sparks' calculations when electrostatic forces were added (the collection efficiency remained at 92%). In our case for a 20 μm diameter particle, the collection efficiency increased from 133 to 141% when electrostatic forces were added to inertial impaction and Brownian diffusion. Our results on the whole differ from those of Sparks. The reason for these differences are probably due to a difference in magnitudes used for the particle and droplet electrostatic charges.

George and Poehlein (1974), Nielsen (1974), and Nielson and Hill (1976) reported single droplet collection efficiencies considering inertial impaction and electrostatic forces. Our results seem to be in general agreement with their results. However, an accurate comparison is not possible because they presented the plots between the single droplet collection efficiencies and the electrostatic parameters for various Stokes numbers (the electrostatic parameter and Stokes number do not specifically establish a given droplet size, particle size and particle and droplet corona charging voltage).

It is difficult to compare the results from the present work with the work done in in cloud physics. Most of the work done in cloud physics deals with drop sizes larger than addressed in this paper. The reported collision efficiencies are mostly for drop–droplet pairs charged or uncharged in an externally applied electric field. Semonin and Plumlee (1966), however, did present some calculations for oppositely charged drop–droplet pairs falling in a field free space. They reported the fractional collision efficiency of a 10 μm dia. particle carrying a charge of 1×10^{-15} C colliding with a 50 μm dia. droplet carrying a charge of 4×10^{-14} C as 8. In our calculations, the fractional collision efficiency of a 10 μm dia. particle carrying a charge of 3×10^{-15} C, colliding with a 50 μm dia. droplet carrying a charge of 1.01×10^{-13} C, was 18.

IV. CONCLUSIONS

Calculated single droplet collection efficiencies considering inertial impaction, Brownian diffusion and electrostatic forces for oppositely charged particle and droplet, indicate that electrostatic forces enhance the particle collection. The higher the droplet and particles are charged, the higher the collection efficiency. It is seen that for the same particle and droplet charging condition, the collection efficiency is larger for smaller droplets which have lower settling velocities. This is due to the larger value of electrostatic parameter owing to the smaller droplet sedimentation velocity. Physically this indicates that when the droplet sedimentation velocity is small, the electrostatic forces have more time to act on the droplet and particle, thereby enhancing the particle collection efficiency.

Acknowledgements – This research was supported in part by the U.S. Environmental Protection Agency Research Grants R-804393 and R-806035 (Dale L. Harmon, Project Officer) and the University of Washington Office of Engineering Research.

REFERENCES

Eads D. K. (1974) M.S. Thesis, University of Illinois.

Einstein A. (1908) *Investigations on the Theory of Brownian Movement*. Dover (1956), from *L'Electrochemie* **19,** 235.

Fonda A. and Herne H. (1960) The classical computations of the aerodynamic capture of particles by spheres. *Int. J. Air. Pollut.* **3,** 26–34.

George H. F. and Poehlein G. W. (1974) Capture of aerosol particles by spherical collectors electrostatic, inertial, interception, and viscous effects. *Envir. Sci. Technol.* **8,** 46–49.

Kramer H. F. and Johnstone H. F. (1955) Collection of aerosol particles in the presence of electrostatic fields. *Ind. Engng Chem.* **47,** 2426–2434.

Johnstone H. F. and Roberts W. H. (1949) Deposition of aerosol particles from moving gas streams. *Ind. Engng Chem.* **41,** 2417–2423.

Langmuir I. (1942) O.S.R.D., Report No. 865.

Langmuir I. (1948) The production of rain by a chain in cumulus clouds at temperatures above freezing. *J. Met.* **5,** 175–192.

Lindblad N. R. and Semonin R. G. (1963) Collision efficiency of cloud droplets in electric fields. *J. geophys. Res.* **68,** 1051–1057.

Moore C. B. and Vannegut B. (1960) Estimates of raindrop collection efficiencies in electrified clouds. *Physics of Precipitation* **5,** AGU, Washington D.C., 291–304.

Nielsen K. A. (1974) Engineering research Institute Technical Report 74127, Iowa State University, Ames, Iowa.

Nielsen K. A. and Hill J. C. (1976) Capture of particles on spheres by inertial and electrical forces. *Ind. Engng Chem. Fund* **15,** 157–163.

Oglesby S., Jr. and Nichols G. B. (1970) A manual of electrostatic precipitation technology – Part I. Fundamentals. Southern Research Institute.

Paluch I. R. (1970) Theoretical collision efficiencies of cloud droplets. *J. geophys. Res.* **75,** 1633–1640.

Pilat M. J., Jaasund S. A. and Sparks L. E. (1974) Collection of aerosol particles by electrostatic droplet scrubbers. *Envir. Sci. Technol.* **8,** 360–362.

Pilat M. J. and Prem A. (1976) Calculated particle collection efficiencies of single droplets including inertial impaction, Brownian diffusion, diffusiphoresis and thermophoresis. *Atmospheric Environment* **10,** 13–19.

Plumlee H. R. and Semonin R. G. (1965) Cloud droplet collision efficiency in electric fields. *Tellus* **17,** 356–364.

Prem A. (1974) M.S. thesis, Department of Civil Engineering, University of Washington.

Ranz W. E. and Wong J. B. (1952) Impaction of dust and smoke particles on surface and body collectors. *Ind. Engng Chem.* **44,** 1371–1381.

Sartor J. D. (1960) Some electrostatic cloud droplet collision efficiencies. *J. geophys. Res.* **65,** 1953–1957.

Sartor J. D. (1970) Accretion rates of cloud drops, raindrops, and small hail in mature thunderstofms. *J. geophys. Res.* **75,** 7547–7558.

Semonin R. G. and Plumlee H. R. (1966) Collision efficiency of charged cloud droplets in electric fields. *J. geophys. Res.* **71,** 4271–4278.

Sparks L. E. (1971) Doctorate dissertation, Department of Civil Engineering, University of Washington.
White H. J. (1963) *Industrial Electrostatic Precipitation.* Addison-Wesley, Reading, Mass.

APPENDIX

DEVELOPMENT OF EQUATIONS OF MOTION FOR A SPHERICAL PARTICLE PAST A SPHERICAL COLLECTOR

A schematic to the model used for calculating single droplet collection efficiency is given in Fig. 1.

From Newton's Second Law

$$m_p . A = F(t) \tag{1}$$

where m_p is the mass of the particle, A is its acceleration and $F(t)$ is the sum of the forces acting on the particle.

$$A = dv_p/dt \tag{2}$$

where v_p is the particle velocity and t is time.

$$F(t) = F_{drag} - F_{ext} \tag{3}$$

where F_{drag} is the force of drag on the particle and F_{ext} is the sum of the external forces acting on the particle.

$$F_{drag} = \frac{6\pi\mu_g R_p}{C}(u - v_p) \tag{4}$$

where u is the fluid velocity, C, the Cunningham correction, μ_g, the gas viscosity and R_p, the particle radius.

$$F_{ext} = F_{Brownian} + F_c + F_{IP} + F_{ID} \tag{5}$$

where $F_{Brownian}$, F_c, F_{IP} and F_{ID} are the forces on the particle due to Brownian diffusion, Coulombic attraction, particle image and droplet image attraction respectively.

Substituting Equations (2), (3) and (4) in (1), we have

$$\frac{dv}{dt} = \frac{6\pi\mu_g R_p}{C . m_p}(u - v) - \frac{F_{ext}}{m_p}. \tag{6}$$

The x and y components of Equation (6) are

$$\frac{dv_x}{dt} = \frac{6\pi\mu_g R_p}{C . m_p}(u_x - v_x) - \frac{F_{ext-x}}{m_p}, \tag{7}$$

$$\frac{dv_y}{dt} = \frac{6\pi\mu_g R_p}{C . m_p}(u_y - v_y) - \frac{F_{ext-y}}{m_p}. \tag{8}$$

Converting Equations (7) and (8) to nondimensional form by the following substitutions

$$X = x/R_d,\ Y = y/R_d,\ V_x = v_x/u_0 = dX/dT,$$
$$V_y = v_y/u_0 = dY/dT,\ T = t . u_0/R_d,\ U_x = u_x/u_0$$
$$U_y = u_y/u_0$$

we have

$$\frac{dV_x}{dT} = \frac{6\pi\mu_g R_p R_d}{C . m_p . u_0}(U_x - V_x) - \frac{F_{ext-x} . R_d}{p_p . u_0^2} \tag{9}$$

$$\frac{dV_y}{dT} = \frac{6\pi\mu_g R_p R_d}{C . m_p . u_0}(U_y - V_y) - \frac{F_{ext-y} . R_d}{m_p . u_0^2}. \tag{10}$$

We know that Stokes number, K, is given as

$$K = \frac{C . m_p . u_0}{12\pi\mu_g R_p . R_d} = \frac{C . \rho_p u_0 R_p^2}{9\mu_g . R_d}. \tag{11}$$

Therefore Equations (9) and (10) can be written as

$$\frac{dV_x}{dT} = \frac{1}{2K}(U_x - V_x) - \frac{F_{ext-x} . R_d}{m_p u_0^2} \tag{12}$$

$$\frac{dV_y}{dT} = \frac{1}{2K}(U_y - V_y) - \frac{F_{ext-y} . R_d}{m_p u_0^2} \tag{13}$$

where R_d is the radius of the droplet, u_0 is the fall speed of the droplet or the undisturbed fluid velocity.

In the model it is assumed that the Brownian force acts only within the film thickness surrounding the water droplet where the particle concentration gradient exists. It was also assumed that all the external forces act radially, that is, they act either towards the center of the droplet or away from it.

$$F_{ext-x} = F_{ext}\cos\theta = F_{ext} . X/(X^2 + Y^2)^{0.5} \tag{14}$$

and

$$F_{ext-y} = F_{ext}\sin\theta = F_{ext} . Y/(X^2 + Y^2)^{0.5} \tag{15}$$

where θ is the angle that the line joining the center of the particle to the center of the droplet makes with the drop centerline.